International Journal of Fluid Machinery and Systems
Vol. 9, No. 3, July-September 2016
DOI: http://dx.doi.org/10.5293/IJFMS.2016.9.3.194
ISSN (Online): 1882-9554

Original Paper

Rotordynamic Characteristics of Floating Ring Seals in Rocket Turbopumps

Yuichiro Tokunaga[1], Hideyuki Inoue[1], Jun Hiromatsu[2], Tetsuya Iguchi[2], Yasuhiro Kuroki[3] and Masaharu Uchiumi[3]

[1] Engineering Research Department, Engineering Division, Eagle Industry Co., Ltd.
1500, Katayanagi, Sakado-shi, Saitama, 350-0285, Japan,
yuuichiro.tokunaga@ekkeagle.com, hideyuki.inoue@ekkegale.com
[2] Engineering Department, Aerospace Division, Eagle Industry Co., Ltd.
1500, Katayanagi, Sakado-shi, Saitama, 350-0285, Japan,
jun.hiromatsu@ekkegale.com, tetsuya.iguchi@ekkegale.com
[3] Research Unit IV, Research and Development Directorate, Japan Aerospace Exploration Agency
1, Koganesawa, Kimigaya, Kakuda, Miyagi, 981-1525, Japan,
kuroki.yasuhiro@jaxa.jp, uchiumi.masaharu@jaxa.jp

Abstract

Floating ring seals offer an opportunity to reduce leakage flows significantly in rotating machinery. Accordingly, they have been applied successfully to rotating machinery within the last several decades. For rocket turbopump applications, fundamental behavior and design philosophy have been revealed. However, further work is needed to explore the rotordynamic characteristics associated with rotor vibrations. In this study, rotordynamic forces for floating ring seals under rotor's whirling motions are calculated to elucidate rotordynamic characteristics. Comparisons between numerical simulation results and experiments demonstrated in our previous report are carried out. The three-dimensional Reynolds equation is solved by the finite-difference method to calculate hydrodynamic pressure distributions and the leakage flow rate. The entrance loss at the upstream inlet of the seal ring is calculated to estimate the Lomakin effect. The friction force at the secondary seal surface is also considered. Numerical simulation results showed that the rotordynamic forces of this type of floating ring seal are determined mainly by the friction force at the secondary seal surface. The seal ring is positioned almost concentrically relative to the rotor by the Lomakin effect. Numerical simulations agree quite well with the experimental results.

Keywords: cryogenics, shaft-seal system, FRS, floating ring seal, dynamic characteristics, rotordynamic coefficient

1. Introduction

Rocket engine turbopumps that operate at high-speed, high-pressure, and high-power conditions suffer from various rotordynamic instability problems. In particular, the lateral vibration of the rotor's whirling motion can cause unwanted direct contact with the rotor surface because of the small clearances of some turbopump components, which can result in severe damage to the turbopumps. Furthermore, rotordynamic fluid forces due to small clearances have a significant impact on rotordynamic stability.

The shaft seal system of a liquid oxygen (LOX) turbopump is one of the critical components of liquid rocket engines. Japanese H-IIA and H-IIB main rocket engines (LE-7A) and a cut-away model of the LE-7 LOX turbopump are shown in Fig. 1. Since the turbine-driven gas is mostly composed of enriched H_2 gas, it must be separated completely from LOX by the seal system in order to prevent hydrogen-oxygen explosions. The schematic of the shaft seal system of an LE-7A LOX turbopump is shown in Fig. 2. Three floating ring seals are used to reduce fluid pressures and leakage from upstream high-pressure regions in the turbopump. A floating ring seal is a non-contact-type rotating shaft seal [1]. It consists mainly of three components: a seal ring floated against a rotor surface, a secondary seal surface, and a spring. These can reduce leakage significantly because of the small gap between their rotors and their seal ring surface compared with conventional annular seals. Accordingly, they have been applied successfully to rotating machinery within the last several decades. The schematics of a floating ring seal for the rocket turbopumps are shown in Fig. 3.

Received February 2 2016; accepted for publication February 11 2016: Review conducted by Shogo Nakamura (Paper number O16002J)
Corresponding author: Yuichiro Tokunaga, yuuichiro.tokunaga@ekkeagle.com

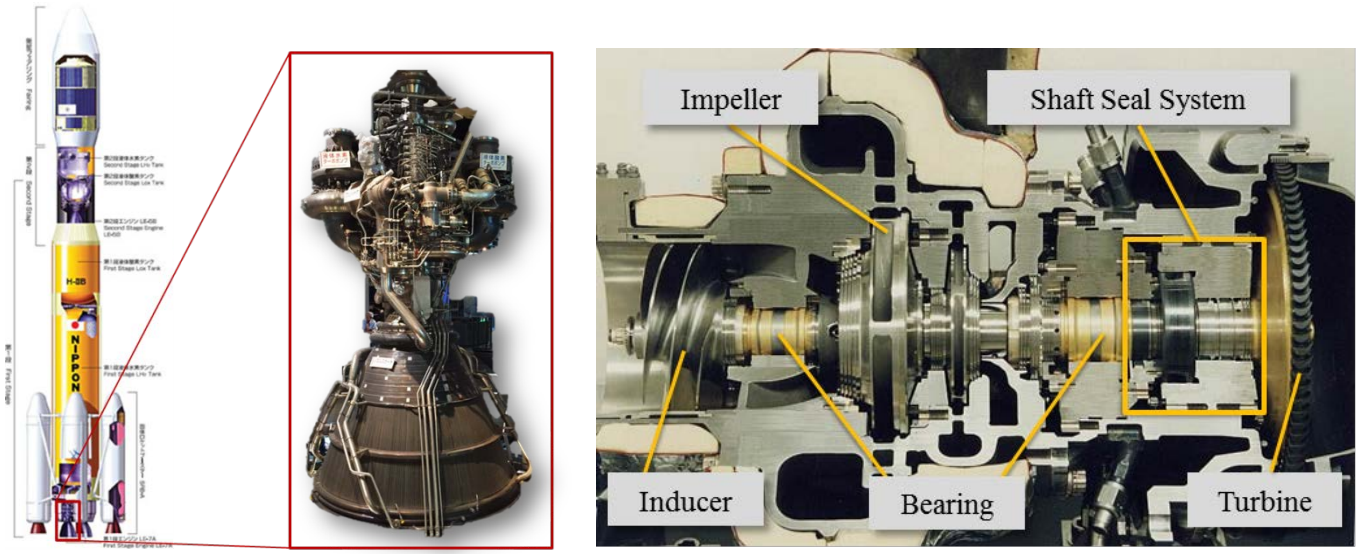

Fig. 1 H-IIA and H-IIB main rocket engine (LE-7A) and cut-away model of the LE-7 LOX turbopump

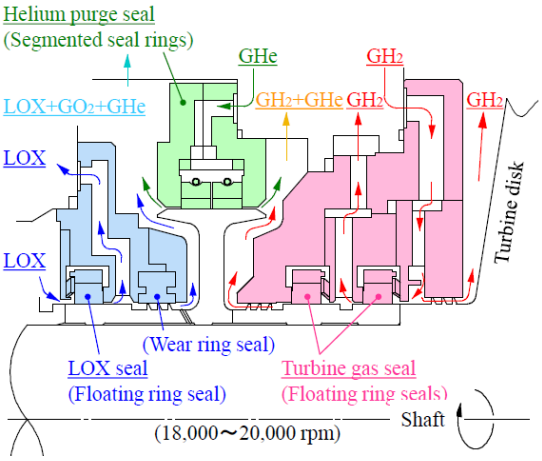

Fig. 2 Shaft-seal system of LE-7A LOX turbopump [2]

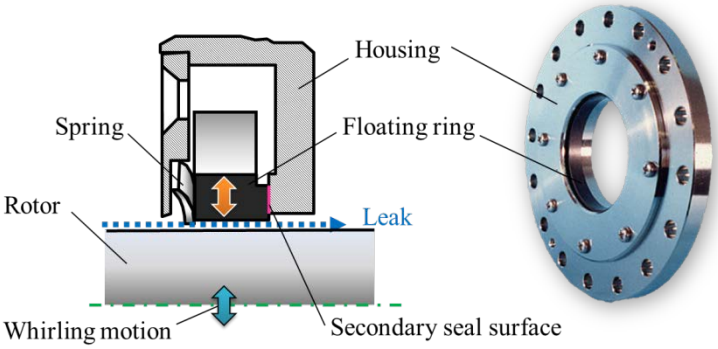

Fig. 3 Schematic of a floating ring seal for a rocket turbopump

A number of studies of rotordynamic instabilities in classical annular seals have been reported [3] [4]. On the other hand, the fundamental characteristics of rotordynamics of floating ring seals have not been fully researched. Further work is needed to explore the rotordynamic characteristics associated with rotor vibrations. In recent studies, the dynamic characteristics of floating ring seals under circular synchronous whirling motion of the rotor have been investigated theoretically and experimentally [5] [6]. However, as far as the authors are aware, few studies have investigated the effect of the relationship between the rotor's spinning speed and the rotor's whirling frequency on the rotordynamic characteristics of floating ring seals.

In our previous report [7], fundamental rotordynamic characteristics of floating ring seals for rocket turbopumps were investigated experimentally. A novel rotordynamic test stand [8] was constructed to measure rotordynamic forces under non-contact state conditions without the influence of other measurement components. The rotor's spinning speed, whirling frequency, and whirling direction can be controlled independently in the test stand.

In this report, rotordynamic forces of floating ring seals under rotor's whirling motions are calculated to elucidate rotordynamic characteristics. Comparisons between results of numerical simulations and experiments demonstrated in our previous report are carried out. The three-dimensional Reynolds equation is solved by the finite-difference method to calculate hydrodynamic pressure distributions and leakage flow rate. The entrance loss at the upstream inlet of the seal surface is calculated to estimate the Lomakin effect [9]. The friction force at the secondary seal surface is also considered.

2. Numerical Calculation

2.1 Rotordynamic Fluid Force

The rotordynamic fluid force caused by the floating ring seal can be decomposed into force in the radial direction F_r, and force in the tangential direction F_t, as shown in Figs. 4 and 5. The positive direction of F_r is defined as the direction outward from the center of the rotor, and the positive direction of F_t is defined as the rotational direction of the rotor. The rotor moves with whirling motion during rotation. The equation of motion and the rotordynamic fluid forces for the floating ring seals can be expressed using the friction force at the secondary seal surfaces:

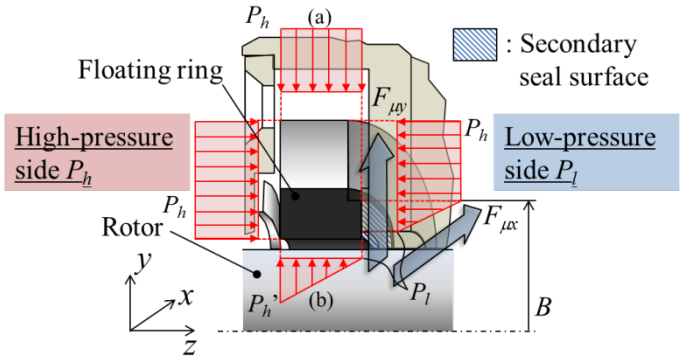

Fig. 4 Pressure distribution acting on a floating ring seal

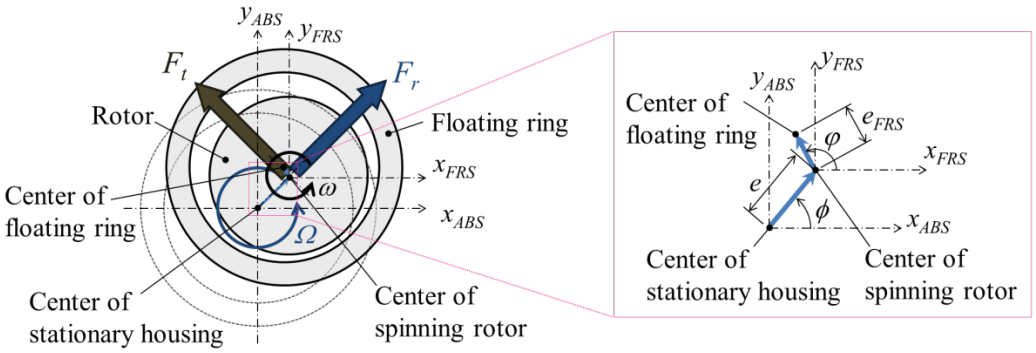

Fig. 5 Schematic of the whirling coordinate system of a floating ring seal

$$\begin{Bmatrix} F_x \\ F_y \end{Bmatrix} = -\begin{bmatrix} M_{xx} & M_{xy} \\ M_{yx} & M_{yy} \end{bmatrix} \begin{Bmatrix} \ddot{x}_{FRS} \\ \ddot{y}_{FRS} \end{Bmatrix} - \begin{bmatrix} C_{xx} & C_{xy} \\ C_{yx} & C_{yy} \end{bmatrix} \begin{Bmatrix} \dot{x}_{FRS} \\ \dot{y}_{FRS} \end{Bmatrix} - \begin{bmatrix} K_{xx} & K_{xy} \\ K_{yx} & K_{yy} \end{bmatrix} \begin{Bmatrix} x_{FRS} \\ y_{FRS} \end{Bmatrix}$$

$$= -\begin{bmatrix} \dfrac{\dot{x}_{ABS}}{|\dot{x}_{ABS}|} & 0 \\ 0 & \dfrac{\dot{y}_{ABS}}{|\dot{y}_{ABS}|} \end{bmatrix} \begin{Bmatrix} F_{\mu x} \\ F_{\mu y} \end{Bmatrix} - \begin{bmatrix} m & 0 \\ 0 & m \end{bmatrix} \begin{Bmatrix} \ddot{x}_{ABS} \\ \ddot{y}_{ABS} \end{Bmatrix} \tag{1}$$

F_r and F_t are calculated with the following equations:

$$\begin{aligned} F_r &= F_x \cos\phi + F_y \sin\phi \\ F_t &= -F_x \sin\phi + F_y \cos\phi \end{aligned} \tag{2}$$

The friction forces at the secondary seal surface $F_{\mu x}$ and $F_{\mu y}$ are calculated with the closing force W_f of the floating ring seal at the secondary seal surface:

$$\begin{aligned} F_{\mu x} &= W_f \mu |\cos\alpha| \\ F_{\mu y} &= W_f \mu |\sin\alpha| \end{aligned} \tag{3}$$

where the friction's acting angle α on the floating ring is:

$$\alpha = \tan^{-1} \frac{\dot{y}_{ABS}}{\dot{x}_{ABS}} \tag{4}$$

The closing force at the secondary seal surface W_f is:

$$W_f = A(P_h - P_l)/2 + W_{SP} \tag{5}$$

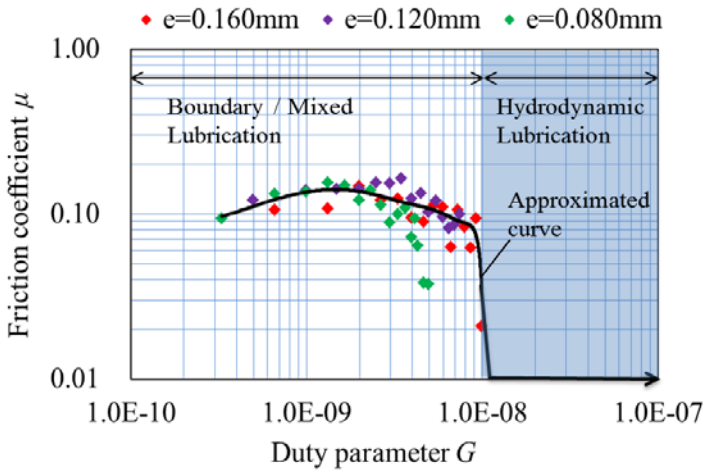

Fig. 6 Stribeck curve approximated by experimentally measured results.

The friction coefficients μ at the secondary seal surface are determined by the Stribeck curve [10] approximated by experimentally measured results in our previous report [7]. The assumed Stribeck curve is shown in Fig. 6. The measured friction coefficients indicate that the floating ring seal contacts the housing at the secondary seal surface mainly in the boundary and the mixed lubrication regions, as shown in Fig. 6. The duty parameter G is calculated by the next equation:

$$G = \eta \frac{2\pi e\Omega}{W_f / B} \tag{6}$$

In the case of friction coefficients in the hydrodynamic lubrication regions, there are few experimental data. Therefore, a constant friction coefficient of 0.01 is applied in the calculation for the hydrodynamic lubrication region. In general, the friction coefficients for hydrodynamic lubrication can be between 0.001 and 0.1; the assumption of 0.01 for the hydrodynamic lubrication is therefore reasonable.

2.2 Pressure distribution

The hydrodynamic pressure distributions at seal surfaces are calculated by solving the Reynolds equation for turbulent flows with the finite-difference method:

$$\frac{\partial}{\partial\theta}\left(G_\theta \frac{\rho h^3}{12\eta}\frac{\partial p}{\partial\theta}\right) + R^2\frac{\partial}{\partial z}\left(G_z \frac{\rho h^3}{12\eta}\frac{\partial p}{\partial z}\right) = \frac{RU}{2}\frac{\partial(\rho h)}{\partial\theta} + \frac{\partial(\rho h)}{\partial t} \tag{7}$$

where, G_θ and G_z are turbulent coefficients proposed by Aoki and Harada [11] [12]:

$$\begin{aligned} \frac{1}{G_\theta} &= 1 + 0.00116 R_h^{\,0.916} \\ \frac{1}{G_z} &= 1 + 0.00120 R_h^{\,0.854} \end{aligned} \tag{8}$$

In this study, the seal surface of the seal ring is assumed to be a flat cylindrical surface without any grooves. Therefore, the seal clearance distributions can be described as follows:

$$h = C\{1 + \varepsilon\cos(\theta - \varphi)\} \tag{9}$$

The conditions for numerical calculations are shown in Table 1. A cylindrical coordinate system is applied for the calculations. The numbers of calculation grids in the axial and circumferential directions are 100 and 150, respectively. Other conditions are determined by experimental conditions.

Table 1 Numerical calculation conditions

Working fluid	Water @ 51degC
Spinning speed ω	1500 rpm
Upstream pressure P_h	0.5, 0.75, 1.0, 1.25 MPaG
Downstream pressure P_l	0 MPaG
Rotor diameter	55.0 mm
Radial seal clearance C	40 μm
Axial length of seal ring L	7.0 mm
Whirling frequency ratio Ω/ω	-1.2 ～ 1.2

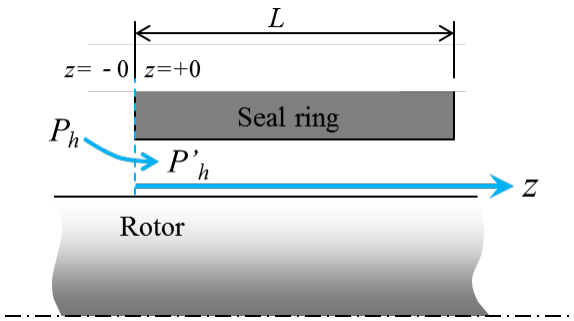

Fig. 7 Schematics of the coordinate system at the seal surface

2.3 Inlet pressure loss

The schematics of the coordinate system at the seal surface are shown in Fig. 7. The inlet pressure losses at the upstream edge of the floating ring seal are calculated with the following equation [12] [13]:

$$P_h' = P_h - \frac{(1+\zeta)}{288}\rho\frac{h^4}{\eta^2}\left(G_z\left.\frac{\partial P}{\partial z}\right|_{z=+0}\right)^2 \tag{10}$$

where ζ is calculated by the next equation approximated from experiments [12][13]:

$$\zeta = -\frac{R_0}{2900} + 2.57 \tag{11}$$

(If R_0<1000, ζ is const.)

The inlet pressure boundary conditions considering inlet pressure losses at the upstream edge are:

$$\begin{cases} p = P_h' \ at \ \ z = +0 \\ p = P_l \ \ at \ \ z = L \end{cases} \tag{12}$$

The average axial velocity at the upstream inlet of the seal surface w_0 is:

$$w_0 = -\frac{h^2}{12\eta}G_z\left.\frac{\partial P}{\partial z}\right|_{z=+0} \tag{13}$$

The magnitude of the Lomakin effect is estimated by calculating the inlet pressure losses at the upstream edge of the seal surface. The leakage flow rates are calculated by the next equation:

$$Q = \int_0^{2\pi}\left[-\frac{Rh^3}{12\eta}G_z\left.\frac{\partial P}{\partial z}\right|_{z=L}\right]d\theta \tag{14}$$

By solving these equations, the rotordynamic forces for floating ring seals, including the friction force at the secondary seal surface, are calculated and compared with experimental results.

3. Results

3.1 Sealing Characteristics

The sealing performance of floating ring seals is investigated theoretically and compared with experimental results. Seal clearance can be deformed by the pressure difference between the outside of the seal ring indicated by (a) in Fig. 4 and the radial seal surface indicated by (b). Therefore, the deformation of the seal clearances at each differential pressure is calculated by FEM analysis in advance. The leakage flow rates are then calculated using seal clearances containing deformations derived from the differential pressures.

The relationship between the spinning speed and leakage rate is shown in Fig. 8. The experimental results indicate that the leakage rate of the floating ring seal is not affected by the spinning speed or the whirling eccentricity. On the other hand, the

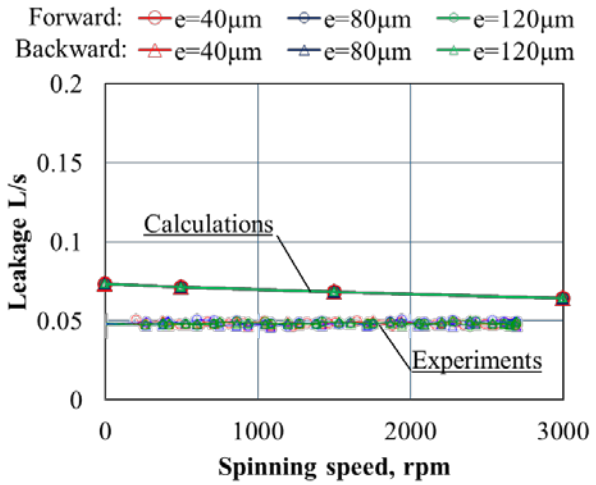

Fig. 8 Relationship between the spinning speed and leakage flow rate (ΔP = 0.5 MPaG, Ω = 15 Hz)

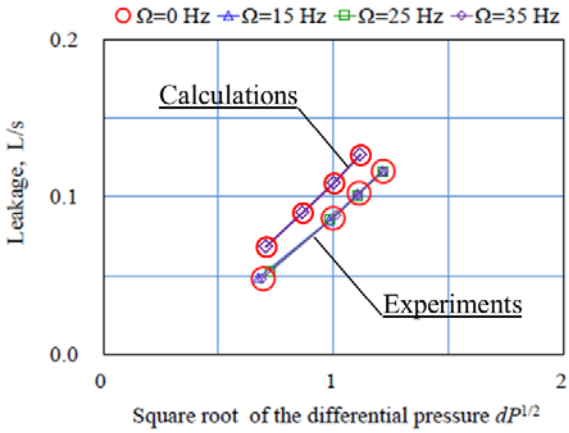

Fig. 9 Relationship between the square root of the differential pressure and leakage flow rate (ω = 1500 rpm, e = 0.12 mm, forward whirling motion, ΔP = 0.5, 0.75, 1.0, 1.25 MPaG)

calculation results of the leakage flow rate show gradual reduction as the spinning speed is increased. The leakage reduction may be caused by increasing flow velocity at the sliding surface. The large flow velocity causes turbulent flow and increases the friction coefficient of the flow. As a result, the reduction of leakage flow rate can be induced. This can be explained similarly by the equations. The large fluid velocity increases the local Reynolds number R_h. From Eq. (8), the turbulent coefficient in the axial direction G_z is decreased. Therefore, from Eqs. (13) and (14), the leakage flow rate Q is also decreased by decreasing the G_z values. A possible reason for constant leakage flows in the experimental results may be derived from the difference between the assumed turbulent coefficients for these calculations and the actual state of the turbulent flows. However, since the effect of the spinning speed ω on the reduction of the leakage flow rate is small and limited, as shown in Fig. 8, the current model could still be reasonable for discussing the fundamental leakage characteristics of floating ring seals.

The relationship between the pressure difference and the leakage rate is shown in Fig. 9. The leakage flow rate increases depending on the increase of the pressure differences. Both the experimental and the calculation results indicate that the leakage flow rate of the floating ring seal is not affected at all by the whirling frequency.

Altogether, the effect of spinning speed on the leakage flow rate is smaller than the effect of the differential pressure. The calculation results in both Figs.8 and 9 are slightly larger than the experimental results. This may be caused by the difference between the assumptions in calculations and the actual conditions of seal clearance, fluid temperature, or turbulent coefficients in experiments. However, the fundamental characteristics of the calculation results agree quite well with those from experiments.

3.2 Rotordynamic Characteristics

The rotordynamic characteristics of the floating ring seals can be evaluated by the force maps of the tangential force F_t and the radial force F_r acting on the rotor during whirling motion. In the case of the tangential force F_t, the negative F_t acting on the rotor with forward whirling motion can suppress the rotor's whirling motion (D in Fig. 10). For the same reason, the positive F_t acting on the rotor with backward whirling motion can also stabilize the rotor (A in Fig. 10). On the other hand, the positive F_t acting on the rotor with forward whirling motion (B in Fig. 10) and the negative F_t acting on the rotor with backward whirling motion (C in Fig. 10) have a destabilizing effect and accelerate the rotor's whirling motion. In the case of the radial force F_r, negative F_r can reduce the whirling eccentricity (F in Fig. 10), which can stabilize the rotor. On the other hand, positive F_r (E in Fig. 10) can increase the whirling eccentricity, which can increase the rotor instability.

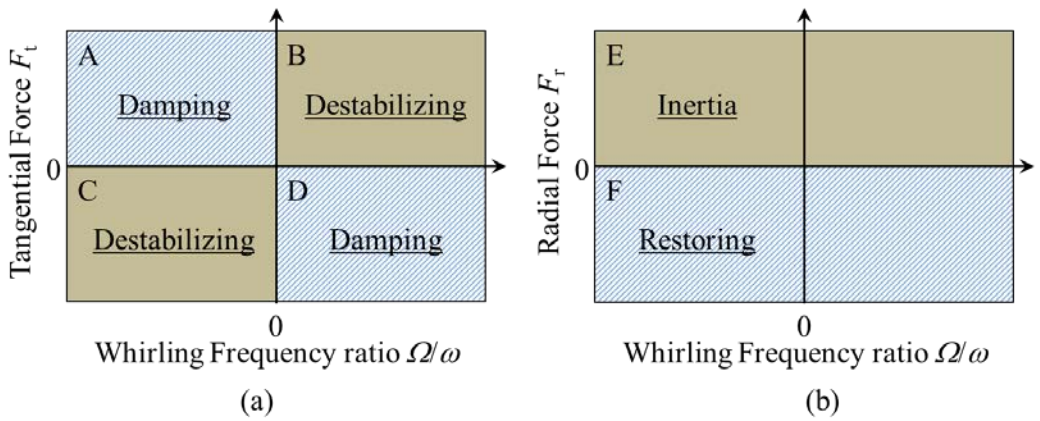

Fig. 10 Schematics of rotordynamic force maps of tangential force F_t and radial force F_r

3.2.1 Effects of Differential Pressure

The increase of differential pressure causes the increase of the friction force at the secondary seal surface. The large friction force at the secondary seal surface may act as a resistance force to suppress the rotor's whirling motion. At the same time, the large friction force prevents repositioning behavior of the seal ring against the rotor. It may cause direct contact of the seal ring with the rotor surface. Therefore, the differential pressure and the friction force at the secondary seal surface could be key factors in determining the rotordynamic characteristics of floating ring seals.

A series of numerical calculations are carried out to investigate the effects of the differential pressure on rotor stability. Figure 11 shows the relationship between the whirling ratio Ω/ω and the tangential force F_t with differential pressures of 0.5, 0.75, 1.0, and 1.25 MPa*G*. This figure shows that the absolute values of the tangential force F_t are increased depending on the increase of differential pressures. The experimental results show same trend as the calculation results.

On the other hand, Fig. 12 shows the relationship between the whirling ratio Ω/ω and the radial force F_r with differential pressures of 0.5, 0.75, 1.0, and 1.25 MPa*G*. The F_r shows a very small negative value close to zero. Therefore, although F_r has a slight stabilization effect, its value is too small to suppress the rotor's whirling motion.

From these results, although the absolute values of the rotordynamic forces F_r and F_t show slight differences between experimental and numerical calculation results, the trends agree quite well.

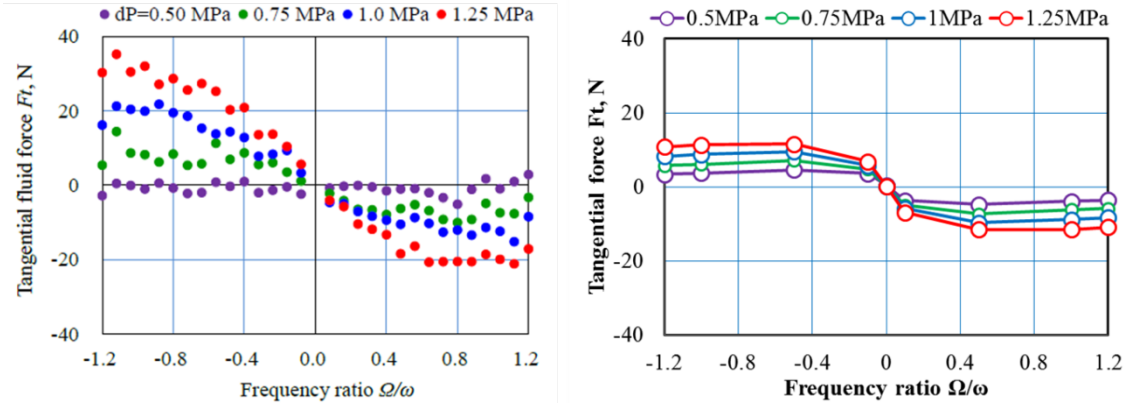

(a) Experimental results (b) Numerical calculations

Fig. 11 Rotordynamic force maps of tangential force F_t (ω = 1500 rpm, e = 0.04 mm)

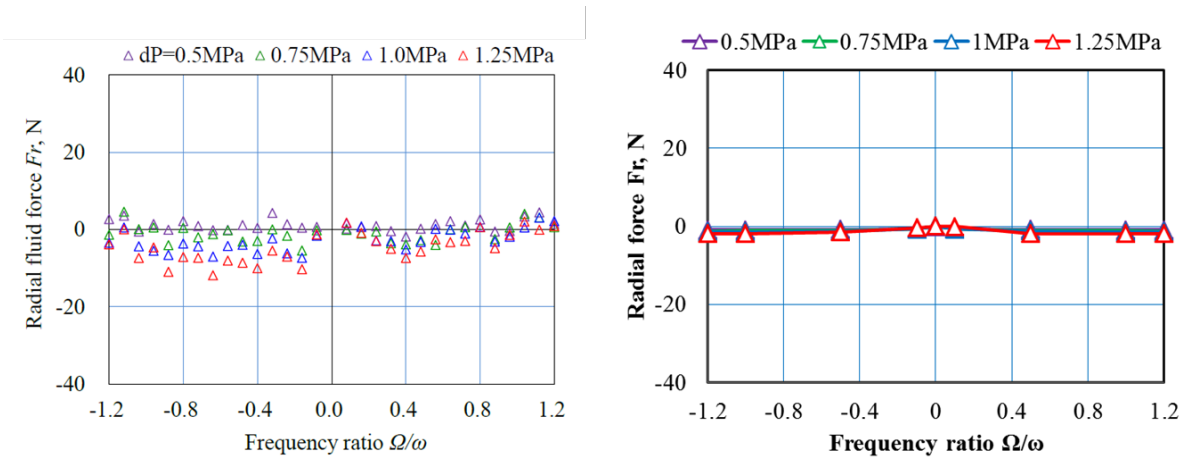

(a) Experimental results (b) Numerical calculations

Fig. 12 Rotordynamic force maps of the radial force F_r (ω = 1500 rpm, e = 0.04 mm)

3.2.2 Effects of Whirl Eccentricity

The rotor's whirling velocity is determined by the eccentricity of the whiling motion and the whirling frequency. Figure 13 shows the relationship between the whirling ratio Ω/ω and the tangential force F_t or the radial force F_r with different whirling eccentricities of 0.04, 0.08, 0.12, and 0.16 mm. In the case of F_t, the results show that the absolute values of F_t are decreased by increasing the whirling eccentricity. Larger whirl eccentricity provides higher sliding velocity at the secondary seal surface. The increase of sliding velocity at the secondary seal surface can induce hydrodynamic lubrication derived from the larger duty parameter *G*, reducing the friction force at the secondary seal surface. As a result, the absolute values of F_t could be reduced by hydrodynamic lubrication. On the other hand, F_r shows a very small negative value close to zero. Therefore, although F_r has a slight stabilization effect, its value is too small to suppress the rotor's whirling motion. From these results, the trends of the numerical calculation results for the rotordynamic forces F_r and F_t agree quite well with the experiments.

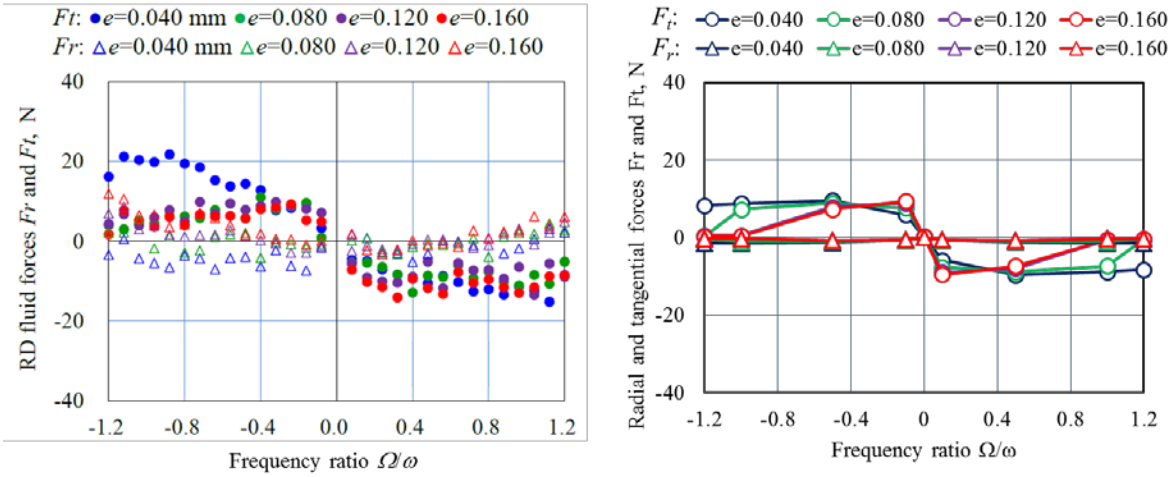

(a) Experimental results (b) Numerical calculations

Fig. 13 Rotordynamic force maps of tangential force F_t and radial force F_r (ω = 1500 rpm, ΔP = 1.0 MPa*G*)

3.2.3 Seal Ring Behavior

The seal ring behavior under the rotor's whirling motion is one of the most important factors affecting significantly not only the stability of the rotor but also the sealing characteristics. Changing the seal clearance during the rotor's whirling motion can cause fluctuation of seal leakage flow. Therefore, the floating ring seal should maintain the initial controlled clearance even under the rotor's whirling motion in order to provide adequate leakage control. The calculation and the experimentally measured results for seal ring behavior under the rotor's whirling motion are shown in Fig. 14. The assumed differential pressure ΔP is 1.25 MPa*G*, the frequency ratio Ω/ω is +1.2, and the whirling eccentricity e is 0.16 mm. The calculated results at the center of the rotor and the seal ring are similar to the experimental results. Moreover, the results indicate that the seal ring is positioned almost concentrically relative to the rotor.

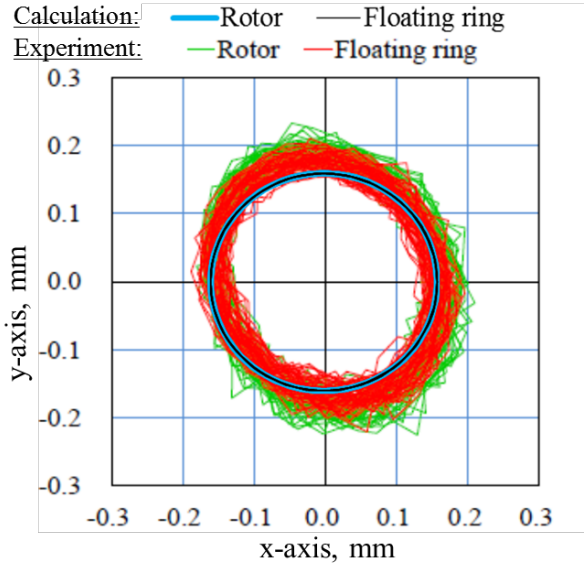

Fig. 14 Orbits of the whirling rotor and the seal ring (ΔP = 1.25 MPa*G*, Ω/ω = +1.2, e = 0.16 mm)

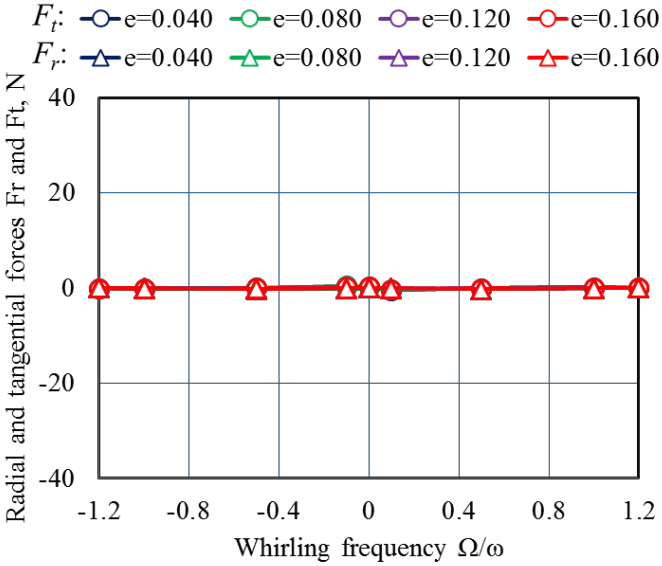

Fig. 15 Rotordynamic force maps of tangential force F_t and radial force F_r regardless of the friction forces at the secondary seal surfaces (ω = 1500 rpm, ΔP = 1.25 MPa*G*)

4. Discussion

4.1 Effects of the Friction Force at the Secondary Seal Surface

According to the results of Fig. 11, the differential pressure affects the rotordynamic characteristics of floating ring seals. Since the friction force at the secondary seal surface is proportional to the differential pressure as indicated in Eqs. (3) and (5), the friction force at the secondary seal surface is an important factor for rotordynamic forces. In order to elucidate the effects of the friction force at the secondary seal surface on rotordynamic forces, a numerical calculation ignoring the friction force at the

secondary seal surface is performed. The calculation results are shown in Fig. 15. As a result, both the tangential force F_t and the radial force F_r become very small (close to zero). Therefore, other factors apart from the friction force, for example, the mass of seal ring m, do not affect rotordynamic stability in this case. This result means that the mass of the seal ring for rocket turbopumps is too small to affect the rotordynamic stability. On the other hand, the large-size floating ring seals [14], such as those applied to power generators in electric power plants, the effect of the mass of the seal ring should be considered.

In any case, for floating ring seals with small mass of seal ring in rocket turbopumps, it is clearly indicated that one of the key factors affecting rotordynamic stability is the friction force at the secondary seal surface. The friction forces tend to act as damping forces to suppress both forward and backward rotor whirling motions.

In order to increase the damping force to stabilize the rotor, the increase of the friction force at the secondary seal surface may be effective. This can be controlled easily by changing the structure of the seal ring. However, this is still challenging because of the difficulty of avoiding direct contact of the seal ring with the rotor surfaces. In addition, thermodynamic effects should be considered when the floating ring seal is operated in cryogenic conditions [15]. Moreover, other parameters such as the mass of the seal ring and the length of the surface structure (e.g. surface texturing, grooves, etc.) should be investigated to propose optimal floating ring seal structures in future studies.

4.2 Contribution of the Lomakin Effect

In order to investigate the contribution of the Lomakin effect to seal ring behavior, a numerical calculation ignoring inlet pressure losses is carried out. The assumed differential pressure ΔP is 1.25 MPaG, the frequency ratio Ω/ω is +1.2, and the whirling eccentricity e is 0.16 mm. The calculation result is shown in Fig. 16. The whirling orbit of the seal ring ignoring inlet pressure losses is not the same orbit as for the rotor's whirling motion. The seal ring is no longer positioned concentrically with the rotor. This result clearly demonstrates that strong repositioning behavior of the floating ring seal can be caused by the Lomakin effect.

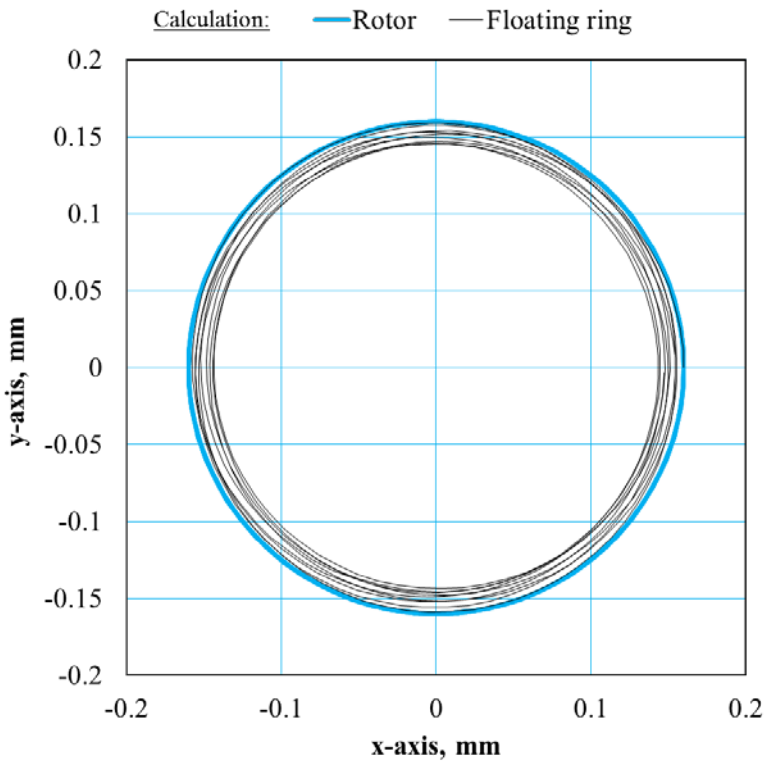

Fig. 16 Calculated orbits of the whirling rotor and the seal ring regardless of the Lomakin effect (ΔP = 1.25 MPaG, Ω/ω = 1.2, e = 0.16 mm)

5. Conclusion

The rotordynamic forces of floating ring seals under rotor whirling motions were calculated to elucidate rotordynamic characteristics. Comparisons between the results of numerical simulations and experiments demonstrated in our previous report were performed. The results of this work are summarized as follows:

1. The effect of spinning speed on leakage flow rate is smaller than the effect of differential pressure. The calculation results are slightly larger than experimental values. This may have been caused by the difference between the assumed seal clearance, fluid temperature, or turbulent coefficients in calculations and the actual conditions in the experiments. However, the fundamental characteristics of the calculation results agree quite well with those of the experiments.

2. In the case of floating ring seals with small mass of seal ring in rocket turbopumps, it is clearly indicated that one of the

key factors affecting rotordynamic stability is the friction force at the secondary seal surface. The friction forces act as damping forces to suppress both forward and backward rotor whirling motions.

3. The calculated orbits of the center of the rotor and the seal ring are similar to those in the experimental results. The results indicate that the seal ring is positioned almost concentrically relative to the rotor. On the other hand, the whirling orbit of the seal ring without considering inlet pressure losses is not the same orbit as for the rotor's whirling motion. As a result, the seal ring is no longer positioned concentrically with the rotor. This result clearly demonstrates that strong repositioning behavior of the floating ring seal can be caused by the Lomakin effect.

Acknowledgments

The investigations were conducted as part of a joint research program of the Japan Aerospace Exploration Agency and Eagle Industry Co., Ltd. The authors gratefully acknowledge the Japan Aerospace Exploration Agency and Eagle Industry Co., Ltd., for their support and permission to publish this paper.

Nomenclature

A	Pressurized area of secondary seal surface [m^2]	Q	Leakage flow rate [m^3/s]
B	Working width in the sliding direction [m]	r, θ, z	Cylindrical coordinates
C	Radial seal clearance [m]	R	Rotor radius [m]
C_{xx}, C_{yy}	Direct damping coefficient term	R_h	Local Reynolds number ($=Uh/\nu$)
C_{xy}, C_{yx}	Cross-coupled damping coefficient term	R_0	Reynolds number for axial flow($=w_0h/\nu$)
e	Absolute whirling eccentricity of rotor [m]	t	Time [s]
e_{FRS}	Eccentricity of the floating ring [m]	U	Sliding velocity [m/s]
F_x, F_y	Rotordynamic fluid forces [N]	w_0	Flow velocity in the axial (z) direction [m/s]
$F_{\mu x}, F_{\mu y}$	Friction force at the secondary seal surface [N]	W_f	Closing force at the secondary seal surface [N]
F_r	Normal fluid force in the radial direction [N]	W_{SP}	Spring force [N]
F_t	Tangential fluid force in the forward whirling direction [N]	x, y, z	Rectangular coordinates
G	Duty parameter	x_{FRS}, y_{FRS}	Relative rectangular coordinates of floating ring from the center of the rotor
G_θ, G_z	Turbulent coefficients	x_{ABS}, y_{ABS}	Absolute rectangular coordinates of floating ring
h	Film thickness [m]		
K_{xx}, K_{yy}	Direct stiffness coefficient term	α	Friction acting angle on the floating ring [rad]
K_{xy}, K_{yx}	Cross-coupled stiffness coefficient term	μ	Friction coefficient
L	Axial seal length [m]	φ	Eccentric angle of the floating ring [rad]
M_{xx}, M_{yy}	Direct added fluid mass coefficient term	ϕ	Eccentric angle of the rotor [rad]
M_{xy}, M_{yx}	Cross-coupled added fluid mass coefficient term	η	Viscosity coefficient [Pa s]
m	Mass of the seal ring [kg]	ν	Dynamic viscosity coefficient ($=\eta/\rho$)
p	Fluid film pressure [Pa]	ε	Eccentricity ratio ($= e_{FRS}/C$)
P_h	Fluid pressure at the upstream side of the seal ring [Pa]	ζ	Inlet loss coefficient
P_h'	Fluid pressure at the upstream side of the seal ring containing the inlet pressure loss [Pa]	Ω	Rotor's whirling frequency [Hz]
P_l	Pressure at the downstream side of the seal ring[Pa]	ω	Rotor's spinning speed [Hz]
ΔP	Differential pressure between P_h and P_l [Pa]	ρ	Fluid density [kg/m^3]

References

[1] NASA, 1978, "Liquid Rocket Engine Turbopump Rotating-Shaft Seals," NASA Space Vehicle Design Criteria (Chemical Propulsion), NASA SP-8121.
[2] Oike, M., Nagao, R., Nosaka, M., Kamijo, K., and Jinnouchi, T., 1995, "Characteristics of a Shaft Seal System for the LE-7 Liquid Oxygen Turbopump," AIAA-95-3102.
[3] Iwatsubo, T., Sheng, B. C., and Matsumoto, T., 1988, "An Experimental Study on the Static and Dynamic Characteristics of Pump Annular Seals," NASA CP 3026, pp. 229-251.
[4] Childs, D., 1993, Turbomachinery Rotordynamics: Phenomena, Modeling, and Analysis, John Wiley & Sons, Inc.
[5] Arghir, M., Nguyen, M., Tonon, D. & Dehouve, J., 2012, "Analytic Modeling of Floating Ring Annular Seals," Journal of Engineering for GasTurbines and Power, 134, pp.052507-1 - 052507-9.
[6] Mariot, A., Arghir, M., Helies, P. & Dehouve, J., 2014, "Experimental and Theoretical Analysis of Floating Ring Annular Seals," 13th EDFIPprime Workshop: Energy Saving in Seals, Futuroscope, October 2, pp. 1-15.
[7] Hiromatsu, J., Uchiumi, M., Takada, S., Inoue, H., Eguchi, M. and Nagao N., "Rotordynamic Fluid Forces of Floating Ring Seal For Rocket Turbopump," ASME IMECE2012-89307.
[8] Eguchi, M. & Maruta, Y., 2003, "Development of Rotordynamics Measurement System with Active Magnetic Bearings," Proceedings of 10th Asia-Pacific Vibration Conference, Gold Coast, Australia, 1, pp.115-120.
[9] Lomakin A., 1958, "Calculation of Critical Number of Revolutions and the Conditions Necessary for Dynamic Stability of Rotors in High-Pressure Hydraulic Machines When Taking Into Account Forces Originating in Sealings," Power and Mechanical Engineering, April, pp.1-5.

[10] Stribeck, R., 1902, “Die Wesentlichen Eigenshanften der Gleit- und Rollenlager,” Zeitschrift des Vereins deutscher Ingenieure, 46, pp.1341-1348, 1432-1438, 1463-1470.
[11] Aoki, H. & M., Harada, 1971, “Turbulent Lubrication Theory for Full Journal Bearings,” (in Japanese), Journal of Japan Society of Lubrication Engineers, 16, 4, pp. 348-356.
[12] Hori, Y., 2006, Hydrodynamic Lubrication, Springer-Verlag Tokyo.
[13] Hori, Y., Fukayama, H. and Kaneko, S., 1985, “Turbulent Lubrication Theory for Annular Plain Seals,” (in Japanese), Journal of Japan Society of Lubrication Engineers, 30, 6, pp.430-437.
[14] Suganami, T., Masuda, T., Oishi, N. & Shimazu, T., 1982, “A Study on Thermal Behavior of Large Seal-Ring,” ASME Journal of Lubrication Technology, 104, pp.449-453.
[15] Oike, M., Nosaka, M., Kikuchi, M. & Hasegawa, S., 1999, “Two-Phase Flow in Floating-Ring Seals for Cryogenic Turbopumps,” Tribology Transactions, 42, 2, pp.273-281.